



The NuSTAR view of radio-quiet AGN

Andrea Marinucci

8th FERRO Meeting
Vnince Hnanice
Sept. 14, 2016



Outline

- Brief introduction
 - Results
- Conclusions

Outline

- Brief introduction

Results

Conclusions and ideas for discussion

Introduction

For the first time in X-ray astronomy, NuSTAR is providing us with high SNR spectra at energies above 10 keV, a crucial energy band for a sound characterization of the underlying physical continuum, and, therefore, for a **tight estimate of the spin of the central BH and high-energy cutoff energy**. Many of the objects studied so far have a **simultaneous coverage** with XMM-Newton/Suzaku and NuSTAR, providing the best data sets so far for this kind of

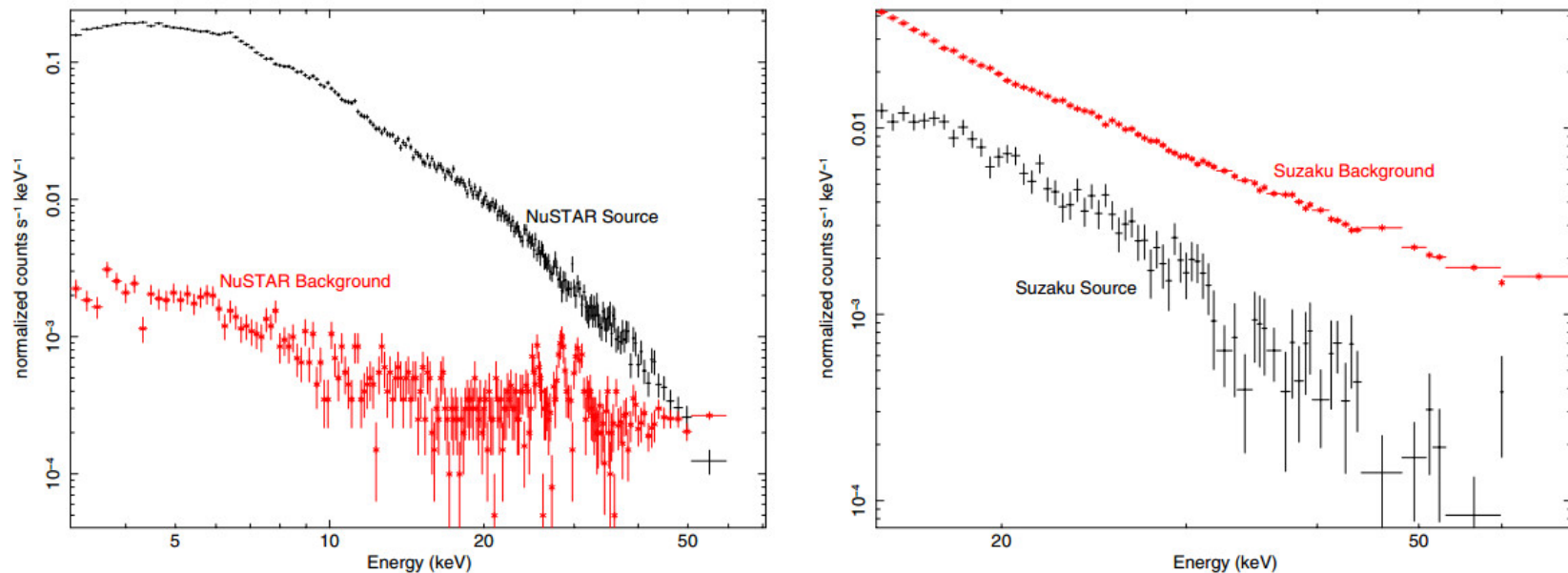
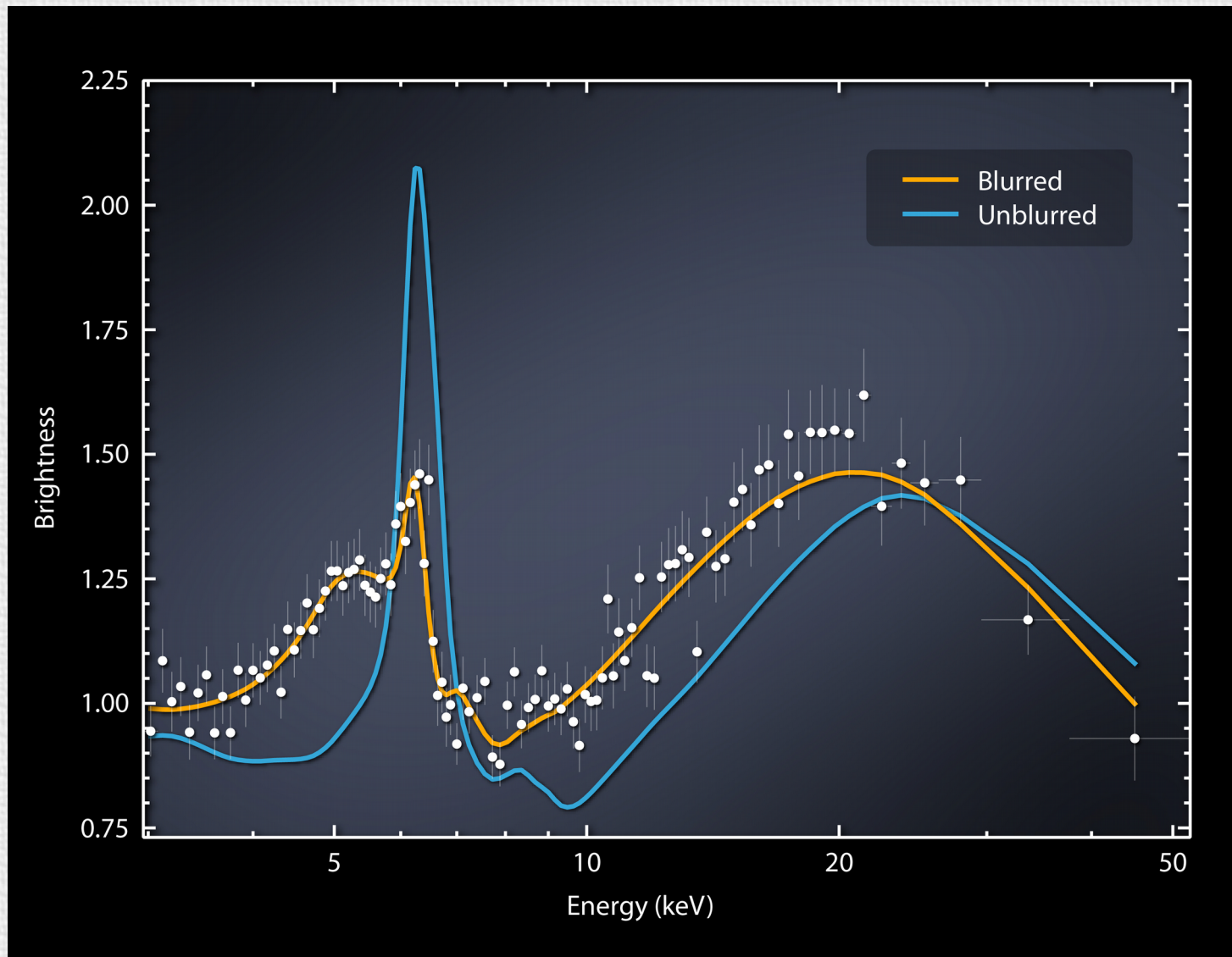


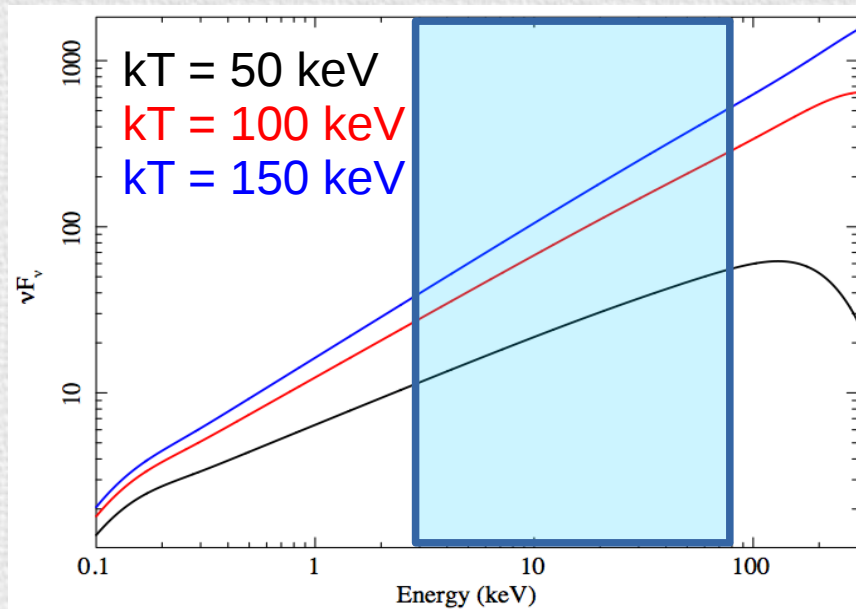
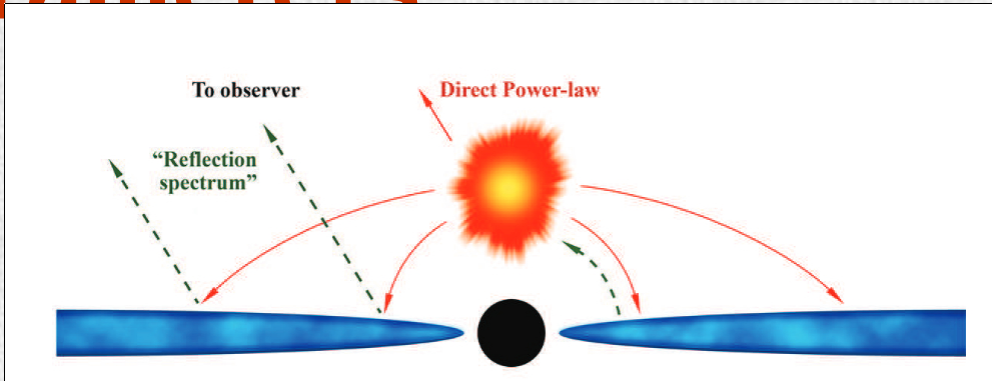
Figure 1. Left: source (in black) + background (in red) spectra from the *NuSTAR* FPMA in the 3–80 keV band. Right: archival *Suzaku* HXD-PIN source (in black) + background (in red) spectra in the 15–70 keV band. The source is at the same 15–70 keV flux level in both observations, within a few percent.

Introduction - Black hole spin measurements

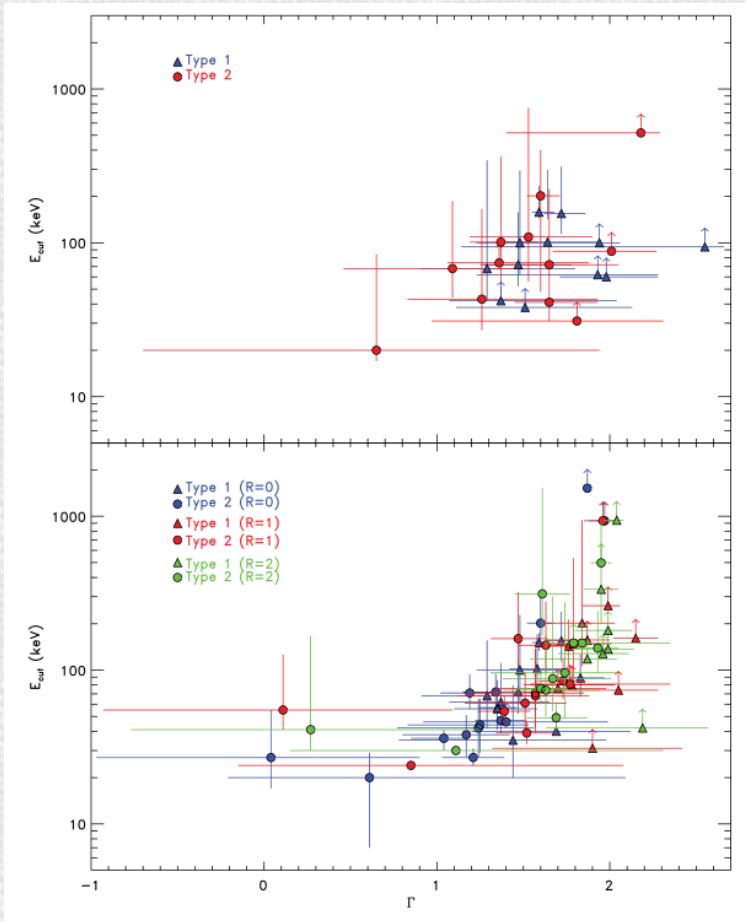
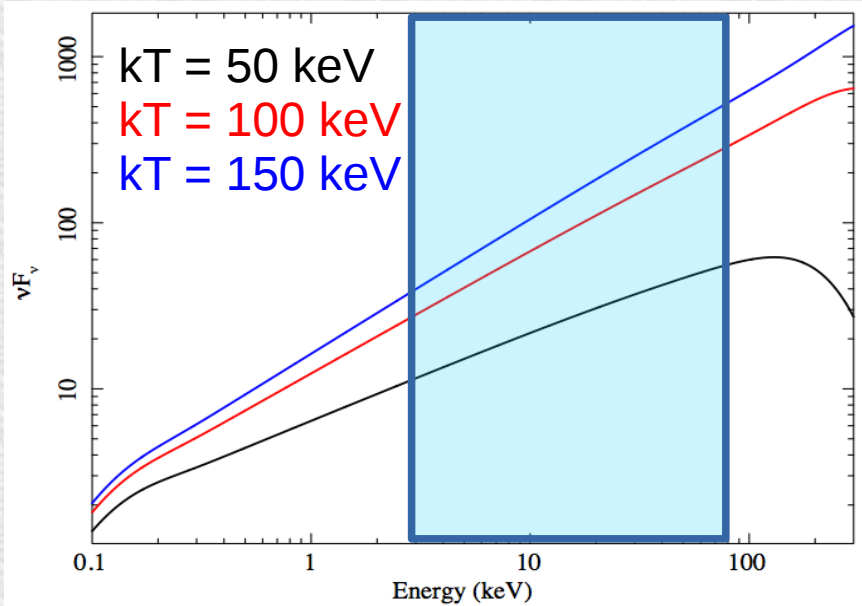
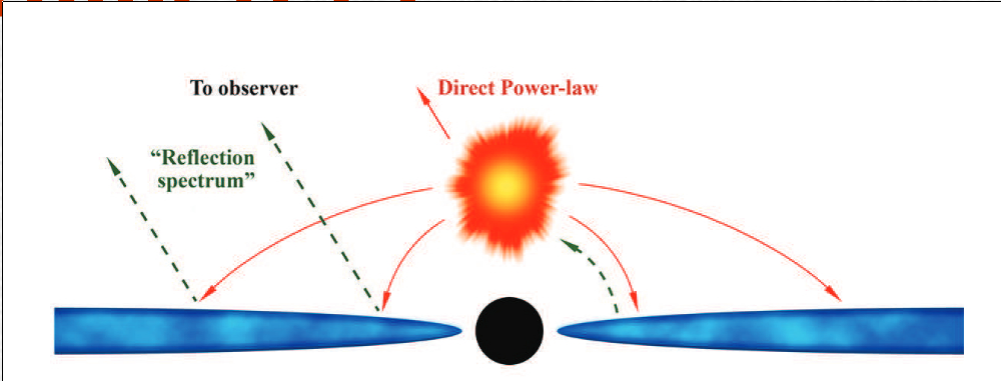


Mrk 335 - NASA/JPL 2014 Press release

Introduction - Coronal parameters



Introduction - Coronal parameters



Molina+2013

Outline

Brief introduction

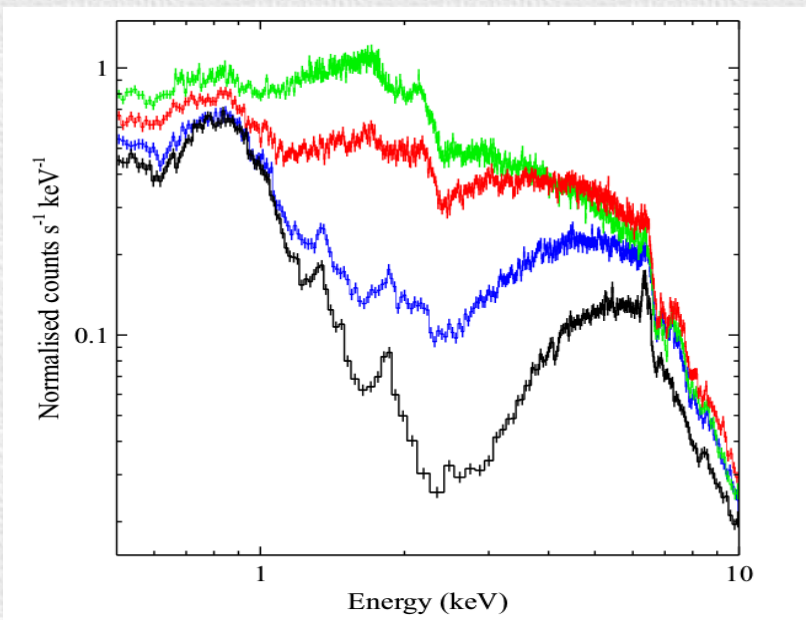
- Results

Conclusions and ideas for discussion

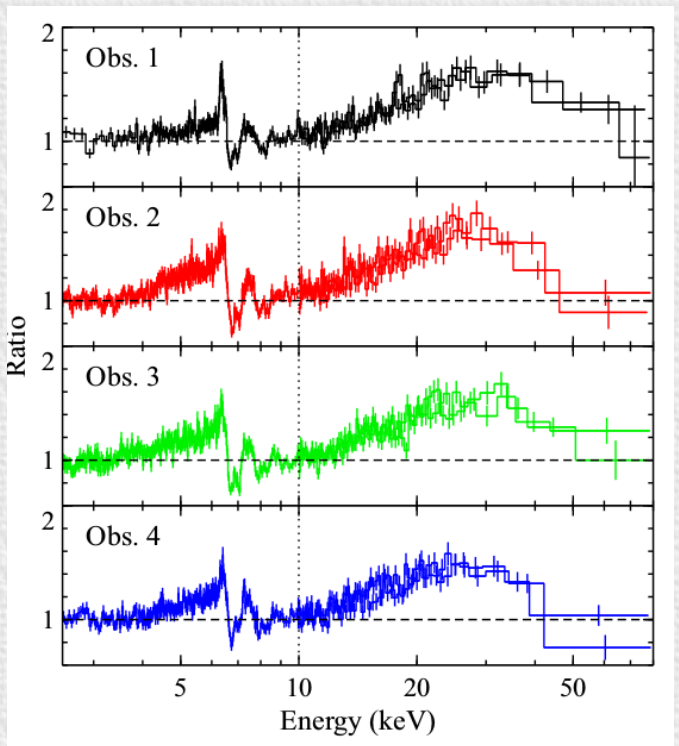
Results - Black hole spin measurements

Target	Spin	Data	Reference
IH0707-495	> 0.988	XMM-Newton/NuSTAR	Kara et al. (2015)
Ark 120	~ 0.5	XMM-Newton/NuSTAR	Matt et al., 2014
Fairall 9	0.973 ± 0.003	XMM-Newton/NuSTAR	Lohfink et al. (2016)
MCG-6-30-15	$0.91^{+0.06}_{-0.07}$	XMM-Newton/NuSTAR	Marinucci et al., 2014a
Mrk 335	> 0.9	Swift/NuSTAR	Parker et al., 2014
NGC 1365	> 0.97	XMM-Newton/NuSTAR	Risaliti et al., 2013 Walton et al., 2014
NGC4151	> 0.9	Suzaku/NuSTAR	Keck et al. (2015)
SWIFT J2127.4	$0.58^{+0.11}_{-0.17}$	XMM-Newton/NuSTAR	Marinucci et al., 2014b

NGC 1365

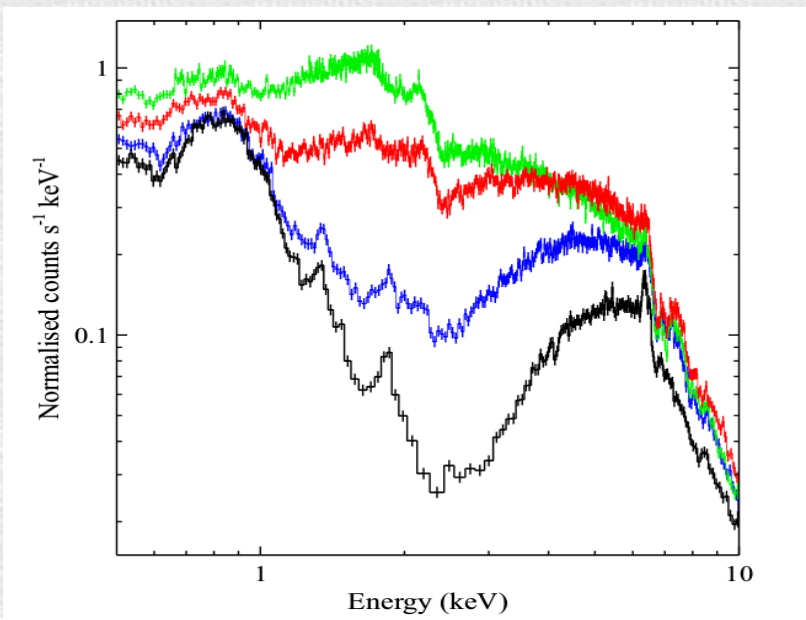


Walton+201
4

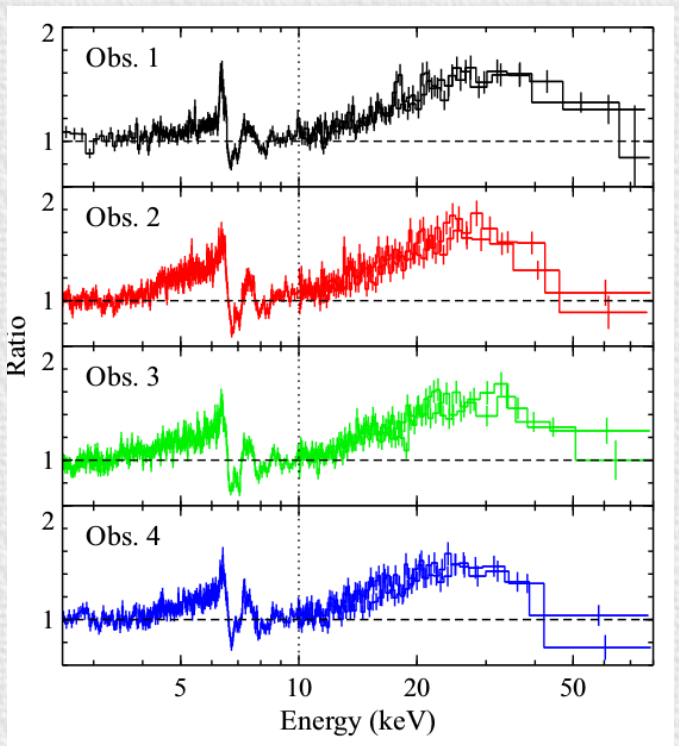


Residuals to a
 $\Gamma=1.75$ power law
continuum

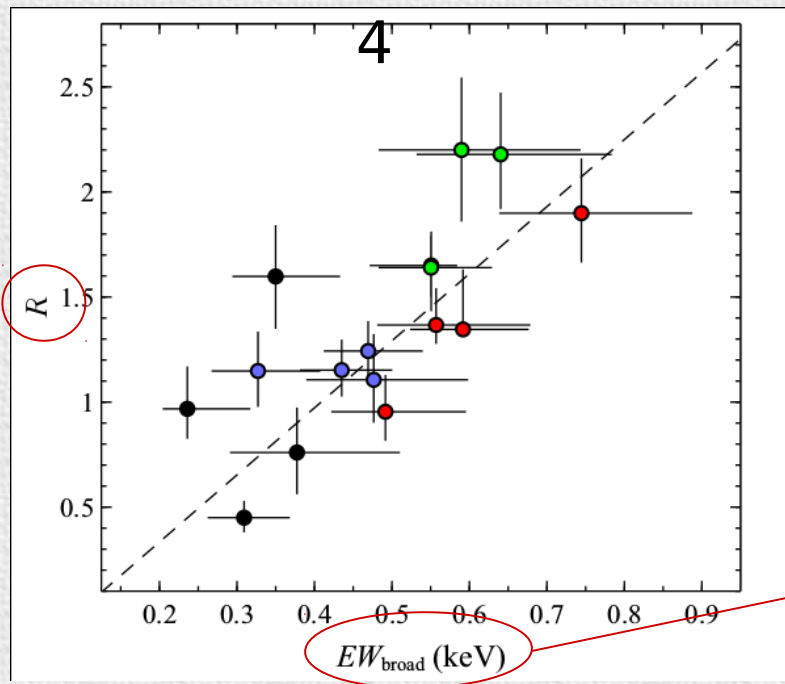
NGC 1365



Walton+201

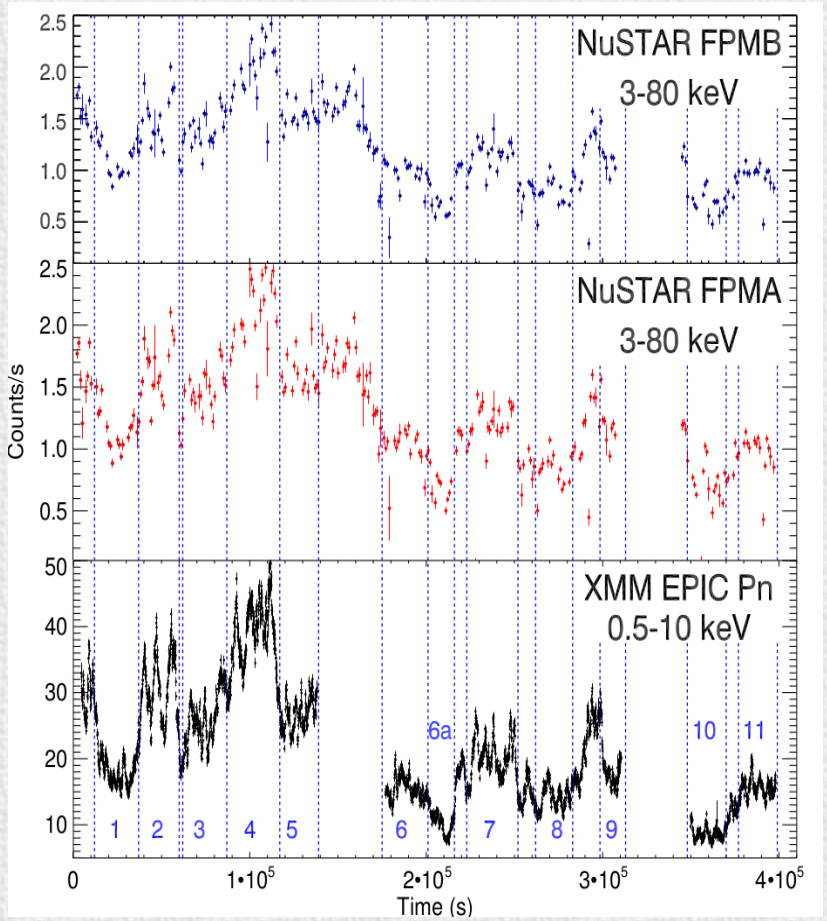


Residuals to a $\Gamma=1.75$ power law continuum



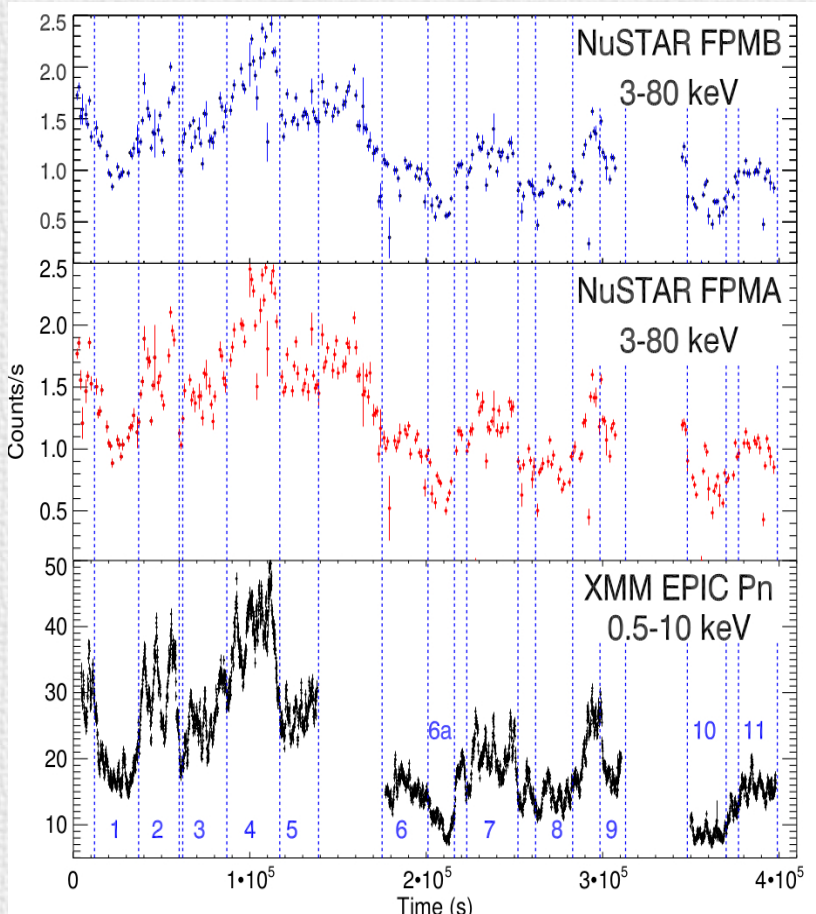
Both parameters indicate a quantity which is relative to the primary continuum

MCG-6-30-16

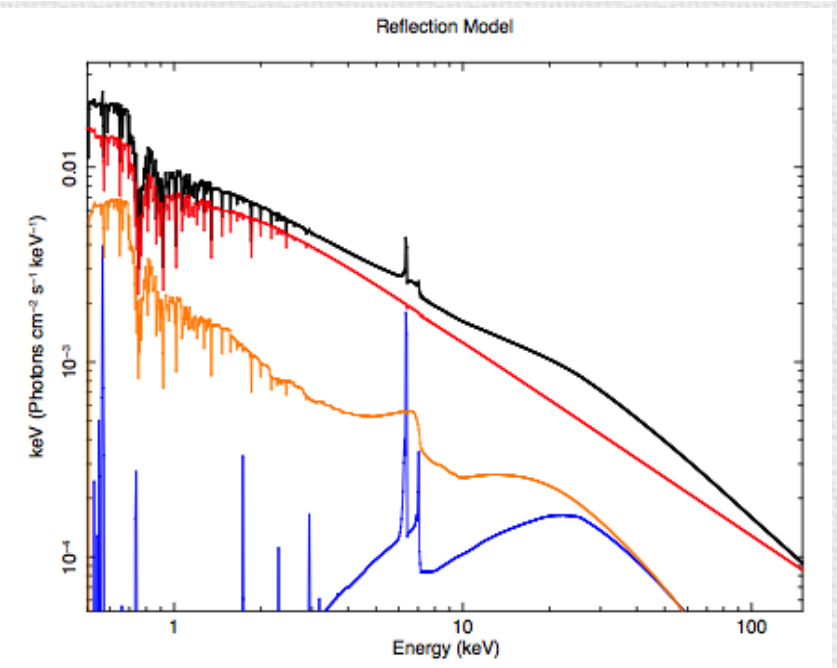
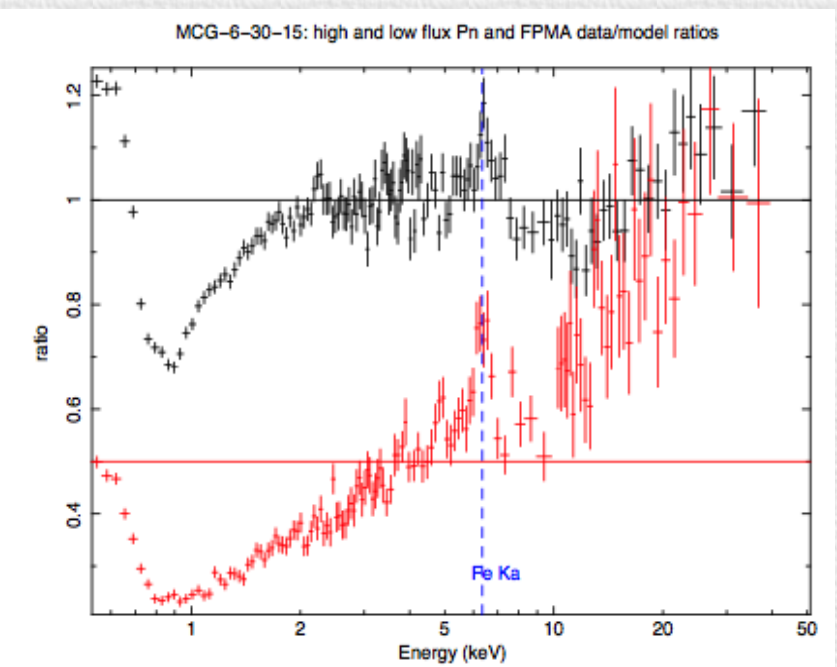


Marinucci+2014

MCG-6-30-16



Marinucci+2014



Results - Coronal parameters

Source	z	$\log(M)$ [M_{\odot}]	r_{co} [r_G]	F_x	E_{cut} [keV]	Γ	Θ	ℓ	Data	References
NGC 5506	0.006	8 ± 1	10	2.9	720^{+130}_{-190}	$1.91^{+0.03}_{-0.03}$	$0.71^{+0.13}_{-0.36}$	4^{+33}_{-3}	SWIFT/NU	1–2
NGC7213	0.006	$7.98^{+0.22}_{-0.24}$	10	0.71	> 240	$1.84^{+0.03}_{-0.03}$	> 0.05	$1.0^{+0.7}_{-0.4}$	NU	3–4
MCG-6-30-15	0.008	6.7 ± 1	2.9	8.2	> 110	$2.061^{+0.005}_{-0.005}$	> 0.04	258^{+232}_{-232}	XMM/NU	5–6
NGC 2110	0.008	8.3 ± 1	10	8.9	> 210	$1.64^{+0.03}_{-0.03}$	> 0.07	10^{+89}_{-9}	SWIFT/NU	7–8
MCG 5-23-16	0.009	7.85 ± 1	10	4.2	116^{+6}_{-5}	$1.85^{+0.01}_{-0.01}$	$0.11^{+0.01}_{-0.04}$	15^{+136}_{-14}	NU	9–11
SWIFT J2127.4+5654	0.014	7.18 ± 1	13	1.1	108^{+11}_{-10}	$2.08^{+0.01}_{-0.01}$	$0.11^{+0.01}_{-0.04}$	34^{+308}_{-31}	XMM/NU	12–13
IC4329A	0.016	8.1 ± 1	10	4.9	186^{+14}_{-14}	$1.73^{+0.01}_{-0.01}$	$0.18^{+0.01}_{-0.07}$	41^{+365}_{-37}	SU/NU	14–15
NGC 5548	0.018	$7.59^{+0.24}_{-0.21}$	4.5	1.3	70^{+40}_{-10}	$1.49^{+0.05}_{-0.05}$	$0.07^{+0.04}_{-0.03}$	88^{+55}_{-37}	XMM/NU	5, 16–17
Mrk 335	0.026	$7.42^{+0.12}_{-0.16}$	3	0.10	> 174	$2.14^{+0.02}_{-0.04}$	> 0.06	36^{+16}_{-9}	SWIFT/NU	18–19
Ark 120	0.033	$7.66^{+0.05}_{-0.06}$	4.4	0.55	> 68	$1.73^{+0.02}_{-0.02}$	> 0.06	4^{+1}_{-1}	XMM/NU	20–21
1H0707-495	0.041	6.31 ± 1	2	0.14	> 63	$3.2^{+0.2}_{-0.2}$	> 0.02	358^{+3219}_{-322}	SWIFT/NU	22–23
Fairall 9	0.047	$8.41^{+0.11}_{-0.09}$	21	0.87	> 242	$1.96^{+0.01}_{-0.02}$	> 0.08	12^{+3}_{-3}	XMM/NU	20, 24
3C390.3	0.056	$9.40^{+0.05}_{-0.06}$	10	1.6	116^{+24}_{-8}	$1.70^{+0.01}_{-0.01}$	$0.11^{+0.02}_{-0.04}$	18^{+3}_{-2}	SU/NU	25–26
Cyg A	0.056	$9.40^{+0.11}_{-0.14}$	10	1.1	> 110	$1.47^{+0.13}_{-0.06}$	> 0.04	6^{+2}_{-1}	NU	27–28
3C382	0.058	9.2 ± 0.5	10	1.4	214^{+147}_{-63}	$1.68^{+0.03}_{-0.02}$	$0.21^{+0.14}_{-0.11}$	12^{+25}_{-8}	SWIFT/NU	29–30

F_x is the 0.1-200 keV X-ray flux in $10^{-10} \text{ erg cm}^{-2} \text{ s}^{-1}$.

References: 1: Guainazzi et al. (2010), 2: Matt et al. (2015), 3: Ursini et al. (2015b), 4: Blank, Harnett & Jones (2005), 5: Emmanoulopoulos et al. (2014), 6: Marinucci et al. (2014c), 7: Moran et al. (2007), 8: Marinucci et al. (2014a), 9: Ponti et al. (2012), 10: Zoghbi et al. (2014), 11: Baloković et al. (2015), 12: Malizia et al. (2008), 13: Marinucci et al. (2014b), 14: Bianchi et al. (2009), 15: Brenneman et al. (2014), 16: Pancoast et al. (2014), 17: Ursini et al. (2015a), 18: Grier et al. (2012), 19: Parker et al. (2014), 20: Peterson et al. (2004), 21: Matt et al. (2014), 22: Bian & Zhao (2003), 23: Kara et al. (2015), 24: Lohfink & Reynolds (2015), 25: Grier et al. (2013), 26: Lohfink & Tombesi (2015), 27: Tadhunter et al. (2003), 28: Reynolds et al. (2015), 29: Winter et al. (2009), 30: Ballantyne et al. (2014)

Fabian+2015

Results - Coronal parameters

Source	z	$\log(M)$ [M_{\odot}]	r_{co} [r_G]	F_x	E_{cut} [keV]	Γ	Θ	ℓ	Data	References
NGC 5506	0.006	8 ± 1	10	2.9	720^{+130}_{-190}	$1.91^{+0.03}_{-0.03}$	$0.71^{+0.13}_{-0.36}$	4^{+33}_{-3}	SWIFT/NU	1–2
NGC7213	0.006	$7.98^{+0.22}_{-0.24}$	10	0.71	> 240	$1.84^{+0.03}_{-0.03}$	> 0.05	$1.0^{+0.7}_{-0.4}$	NU	3–4
MCG-6-30-15	0.008	6.7 ± 1	2.9	8.2	> 110	$2.061^{+0.005}_{-0.005}$	> 0.04	258^{+232}_{-232}	XMM/NU	5–6
NGC 2110	0.008	8.3 ± 1	10	8.9	> 210	$1.64^{+0.03}_{-0.03}$	> 0.07	10^{+89}_{-9}	SWIFT/NU	7–8
MCG 5-23-16	0.009	7.85 ± 1	10	4.2	116^{+6}_{-5}	$1.85^{+0.01}_{-0.01}$	$0.11^{+0.01}_{-0.04}$	15^{+136}_{-14}	NU	9–11
SWIFT J2127.4+5654	0.014	7.18 ± 1	13	1.1	108^{+11}_{-10}	$2.08^{+0.01}_{-0.01}$	$0.11^{+0.01}_{-0.04}$	34^{+308}_{-31}	XMM/NU	12–13
IC4329A	0.016	8.1 ± 1	10	4.9	186^{+14}_{-14}	$1.73^{+0.01}_{-0.01}$	$0.18^{+0.01}_{-0.07}$	41^{+365}_{-37}	SU/NU	14–15
NGC 5548	0.018	$7.59^{+0.24}_{-0.21}$	4.5	1.3	70^{+40}_{-10}	$1.49^{+0.05}_{-0.05}$	$0.07^{+0.04}_{-0.03}$	88^{+55}_{-37}	XMM/NU	5, 16–17
Mrk 335	0.026	$7.42^{+0.12}_{-0.16}$	3	0.10	> 174	$2.14^{+0.02}_{-0.04}$	> 0.06	36^{+16}_{-9}	SWIFT/NU	18–19
Ark 120	0.033	$7.66^{+0.05}_{-0.06}$	4.4	0.55	> 68	$1.73^{+0.02}_{-0.02}$	> 0.06	4^{+1}_{-1}	XMM/NU	20–21
1H0707-495	0.041	6.31 ± 1	2	0.14	> 63	$3.2^{+0.2}_{-0.2}$	> 0.02	358^{+3219}_{-322}	SWIFT/NU	22–23
Fairall 9	0.047	$8.41^{+0.11}_{-0.09}$	21	0.87	> 242	$1.96^{+0.01}_{-0.02}$	> 0.08	12^{+3}_{-3}	XMM/NU	20, 24
3C390.3	0.056	$9.40^{+0.05}_{-0.06}$	10	1.6	116^{+24}_{-8}	$1.70^{+0.01}_{-0.01}$	$0.11^{+0.02}_{-0.04}$	18^{+3}_{-2}	SU/NU	25–26
Cyg A	0.056	$9.40^{+0.11}_{-0.14}$	10	1.1	> 110	$1.47^{+0.13}_{-0.06}$	> 0.04	6^{+2}_{-1}	NU	27–28
3C382	0.058	9.2 ± 0.5	10	1.4	214^{+147}_{-63}	$1.68^{+0.03}_{-0.02}$	$0.21^{+0.14}_{-0.11}$	12^{+25}_{-8}	SWIFT/NU	29–30

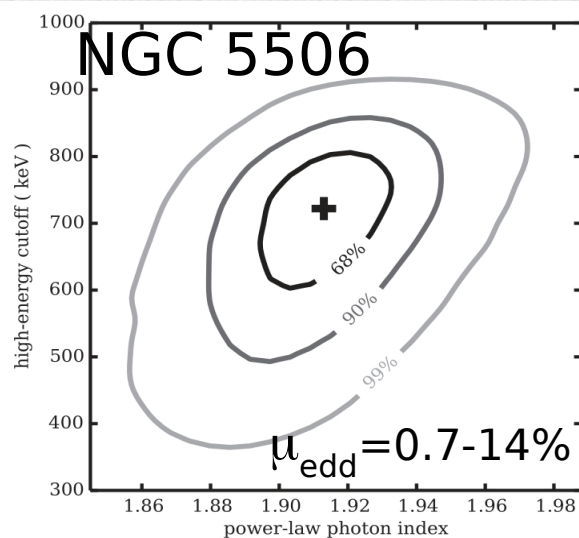
F_x is the 0.1-200 keV X-ray flux in $10^{-10} \text{ erg cm}^{-2} \text{ s}^{-1}$.

References: 1: Guainazzi et al. (2010), 2: Matt et al. (2015), 3: Ursini et al. (2015b), 4: Blank, Harnett & Jones (2005), 5: Emmanoulopoulos et al. (2014), 6: Marinucci et al. (2014c), 7: Moran et al. (2007), 8: Marinucci et al. (2014a), 9: Ponti et al. (2012), 10: Zoghbi et al. (2014), 11: Baloković et al. (2015), 12: Malizia et al. (2008), 13: Marinucci et al. (2014b), 14: Bianchi et al. (2009), 15: Brenneman et al. (2014), 16: Pancoast et al. (2014), 17: Ursini et al. (2015a), 18: Grier et al. (2012), 19: Parker et al. (2014), 20: Peterson et al. (2004), 21: Matt et al. (2014), 22: Bian & Zhao (2003), 23: Kara et al. (2015), 24: Lohfink & Reynolds (2015), 25: Grier et al. (2013), 26: Lohfink & Tombesi (2015), 27: Tadhunter et al. (2003), 28: Reynolds et al. (2015), 29: Winter et al. (2009), 30: Ballantyne et al. (2014)

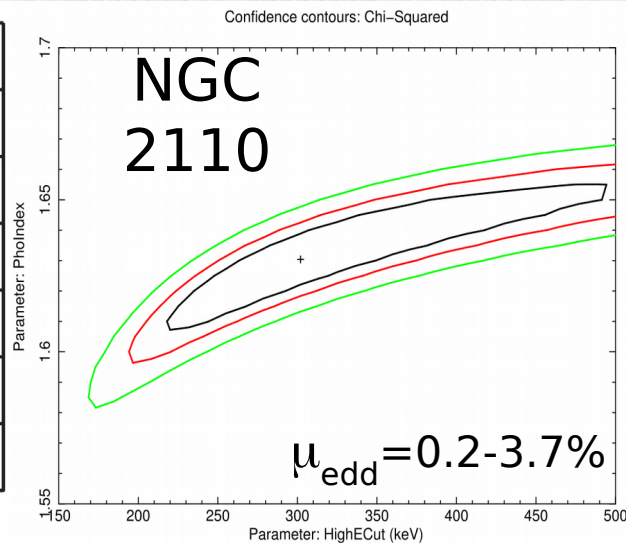
Fabian+2015

Results - Coronal parameters

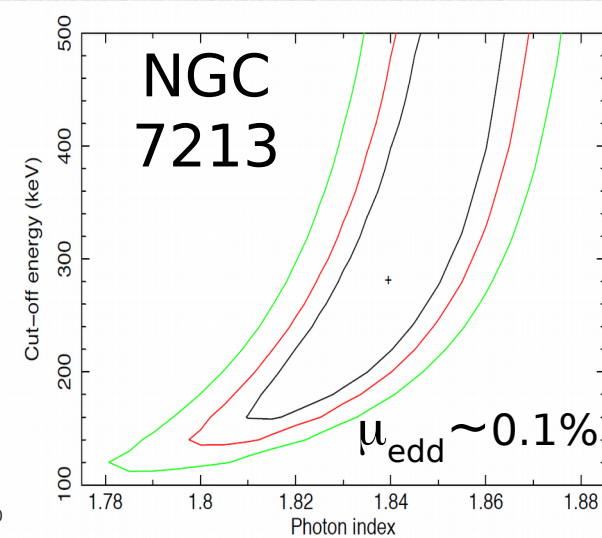
In some bright sources, high values or lower limits to the cutoff energy have been found, suggesting the presence of a very hot corona surrounding the accretion disc.



Matt+15



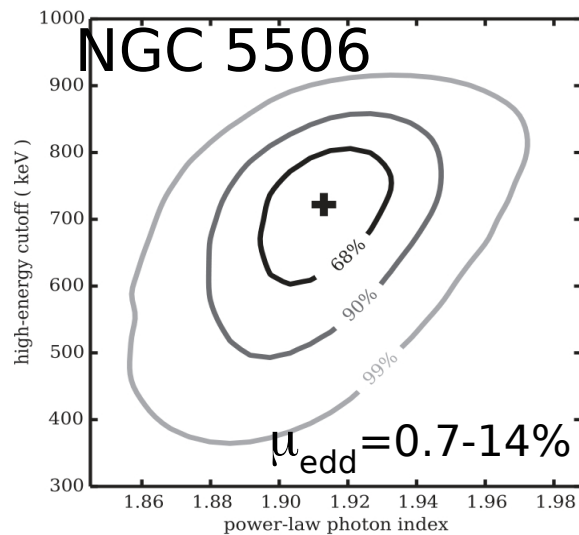
Marinucci+15



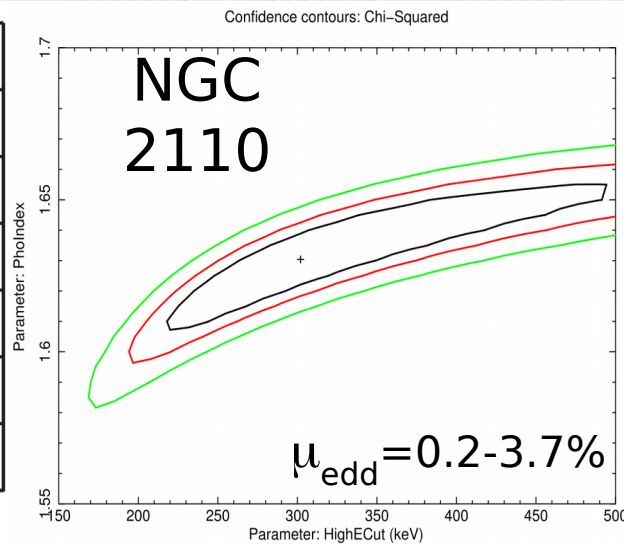
Ursini+15

Results - Coronal parameters

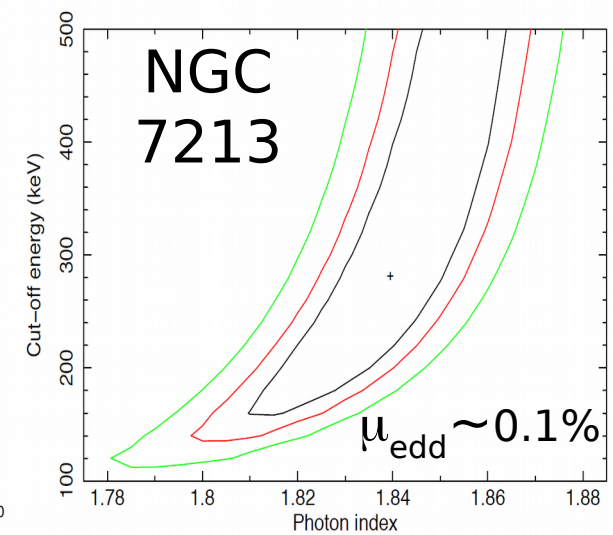
In some bright sources, high values or lower limits to the cutoff energy have been found, suggesting the presence of a very hot corona surrounding the accretion disc.



Matt+15



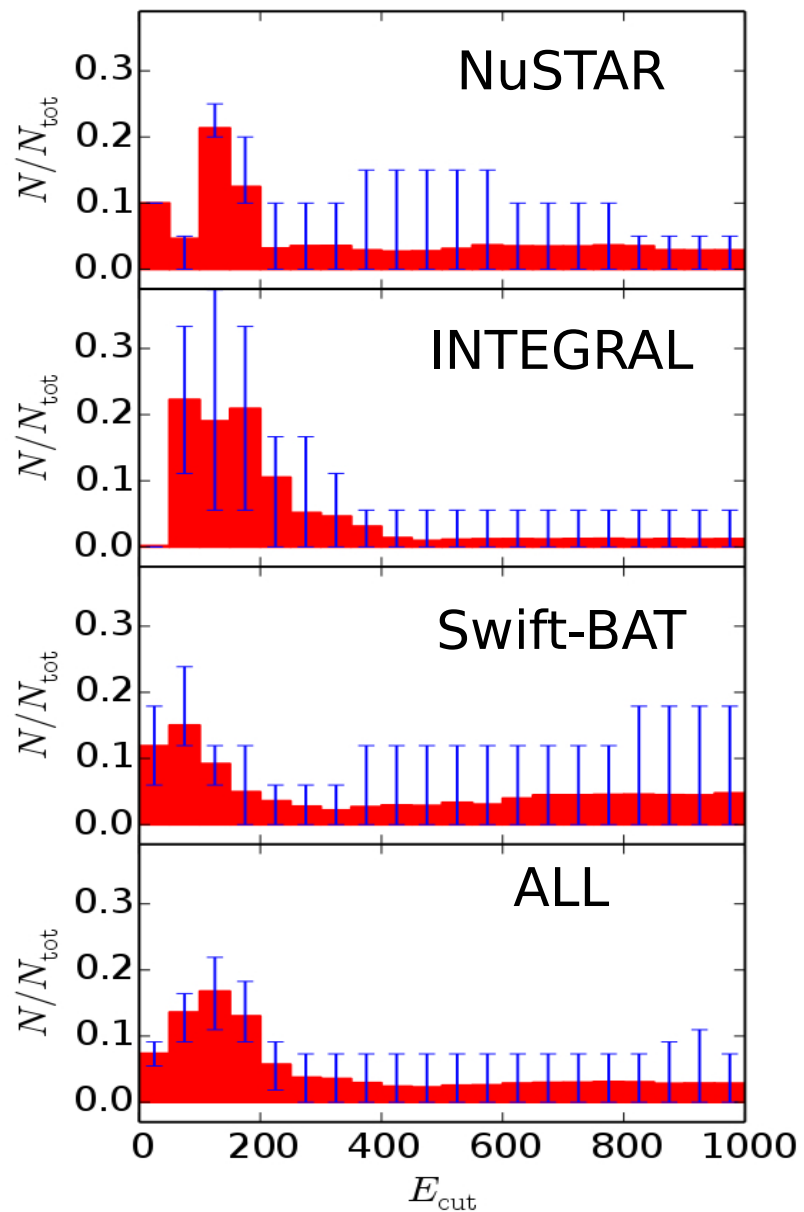
Marinucci+15



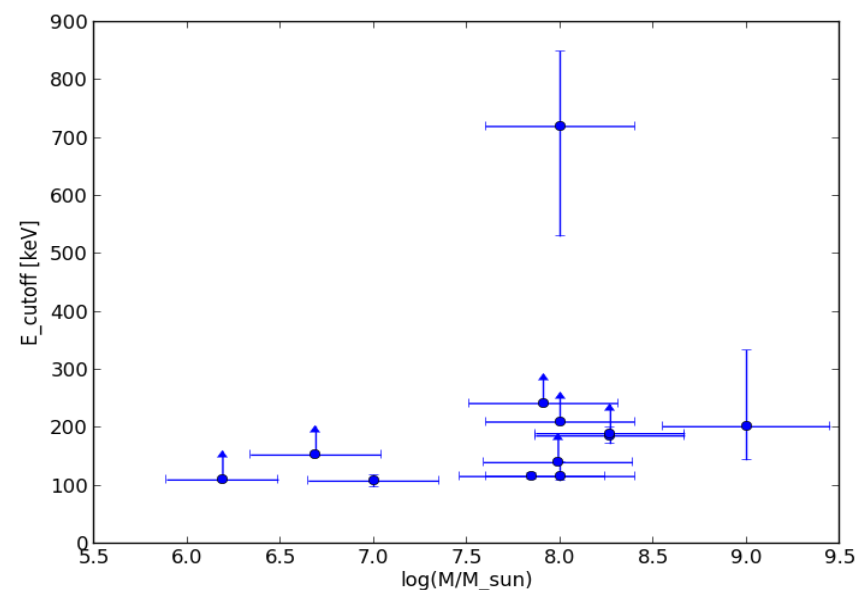
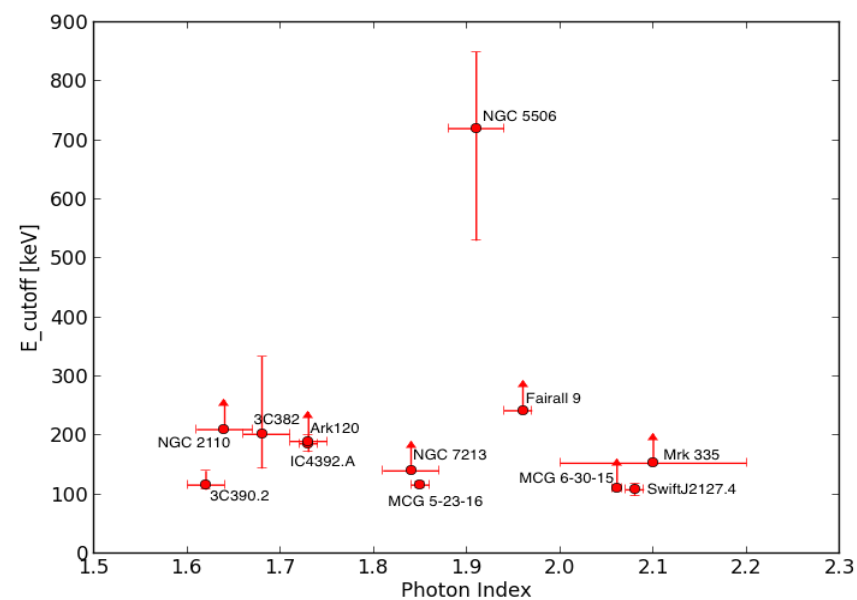
Ursini+15

The next step is to build a small catalog and to start looking for correlations between the coronal temperature and other physical properties (e.g. black hole mass, accretion rate).

Results - Coronal parameters



Fabian+15



Tortosa et al., in prep.

Results - Coronal parameters

Source	z	$\log(M)$ [M_{\odot}]	r_{co} [r_G]	F_x	E_{cut} [keV]	Γ	Θ	ℓ	Data	References
NGC 5506	0.006	8 ± 1	10	2.9	720^{+130}_{-190}	$1.91^{+0.03}_{-0.03}$	$0.71^{+0.13}_{-0.36}$	4^{+33}_{-3}	SWIFT/NU	1–2
NGC7213	0.006	$7.98^{+0.22}_{-0.24}$	10	0.71	> 240	$1.84^{+0.03}_{-0.03}$	> 0.05	$1.0^{+0.7}_{-0.4}$	NU	3–4
MCG-6-30-15	0.008	6.7 ± 1	2.9	8.2	> 110	$2.061^{+0.005}_{-0.005}$	> 0.04	258^{+232}_{-232}	XMM/NU	5–6
NGC 2110	0.008	8.3 ± 1	10	8.9	> 210	$1.64^{+0.03}_{-0.03}$	> 0.07	10^{+89}_{-9}	SWIFT/NU	7–8
MCG 5-23-16	0.009	7.85 ± 1	10	4.2	116^{+6}_{-5}	$1.85^{+0.01}_{-0.01}$	$0.11^{+0.01}_{-0.04}$	15^{+136}_{-14}	NU	9–11
SWIFT J2127.4+5654	0.014	7.18 ± 1	13	1.1	108^{+11}_{-10}	$2.08^{+0.01}_{-0.01}$	$0.11^{+0.01}_{-0.04}$	34^{+308}_{-31}	XMM/NU	12–13
IC4329A	0.016	8.1 ± 1	10	4.9	186^{+14}_{-14}	$1.73^{+0.01}_{-0.01}$	$0.18^{+0.01}_{-0.07}$	41^{+365}_{-37}	SU/NU	14–15
NGC 5548	0.018	$7.59^{+0.24}_{-0.21}$	4.5	1.3	70^{+40}_{-10}	$1.49^{+0.05}_{-0.05}$	$0.07^{+0.04}_{-0.03}$	88^{+55}_{-37}	XMM/NU	5, 16–17
Mrk 335	0.026	$7.42^{+0.12}_{-0.16}$	3	0.10	> 174	$2.14^{+0.02}_{-0.04}$	> 0.06	36^{+16}_{-9}	SWIFT/NU	18–19
Ark 120	0.033	$7.66^{+0.05}_{-0.06}$	4.4	0.55	> 68	$1.73^{+0.02}_{-0.02}$	> 0.06	4^{+1}_{-1}	XMM/NU	20–21
1H0707-495	0.041	6.31 ± 1	2	0.14	> 63	$3.2^{+0.2}_{-0.2}$	> 0.02	358^{+3219}_{-322}	SWIFT/NU	22–23
Fairall 9	0.047	$8.41^{+0.11}_{-0.09}$	21	0.87	> 242	$1.96^{+0.01}_{-0.02}$	> 0.08	12^{+3}_{-3}	XMM/NU	20, 24
3C390.3	0.056	$9.40^{+0.05}_{-0.06}$	10	1.6	116^{+24}_{-8}	$1.70^{+0.01}_{-0.01}$	$0.11^{+0.02}_{-0.04}$	18^{+3}_{-2}	SU/NU	25–26
Cyg A	0.056	$9.40^{+0.11}_{-0.14}$	10	1.1	> 110	$1.47^{+0.13}_{-0.06}$	> 0.04	6^{+2}_{-1}	NU	27–28
3C382	0.058	9.2 ± 0.5	10	1.4	214^{+147}_{-63}	$1.68^{+0.03}_{-0.02}$	$0.21^{+0.14}_{-0.11}$	12^{+25}_{-8}	SWIFT/NU	29–30
⋮										
GRS 1734-292	0.021	8.9 ± 0.7	10	2.1	58^{+24}_{-7}	$1.55^{+0.15}_{-0.08}$	$0.06^{+0.02}_{-0.02}$	5^{+20}_{-4}	XMM/INT/BAT/NU	
MCG+8-11-11						?	?			
Swift/NU										
NGC 6814						?	?			Swit/NU

More observations are under scrutiny ..

Outline

Brief Introduction

Results

- Conclusions

Conclusions

- A number of robust black hole spin measurements have been presented since the launch of NuSTAR
- Following the continuum helps in keeping track of the broad Iron $K\alpha$ component
- High energy cut-off have been measured in several AGN with NuSTAR (more are yet to come!)
 - They are not ubiquitous
- Further observations will help us in understanding the nature of the primary continuum, such as the relation between the accretion rate and the cutoff energy and the link between the disc reflection and the extension of the hot corona.